processes

MDPI

Article

Modification Effects of High-Pressure Homogenization and Decolorization on Microalgae-Fortified 3D-Printed Foods

Dalne Sinclair [1], Armin Mirzapour-Kouhdasht [1,2], Juan A. Velasquez [1,2], Da Chen [1], Senay Simsek [1] and Jen-Yi Huang [1,2,3,*]

[1] Department of Food Science, Purdue University, 745 Agriculture Mall Drive, West Lafayette, IN 47907, USA; sinclai5@purdue.edu (D.S.); mirzapourkouhdasht.1@osu.edu (A.M.-K.); velasquez.134@osu.edu (J.A.V.); chen3370@purdue.edu (D.C.); ssimsek@purdue.edu (S.S.)
[2] Department of Food Science and Technology, The Ohio State University, 2015 Fyffe Road, Columbus, OH 43210, USA
[3] Department of Food, Agricultural and Biological Engineering, The Ohio State University, 590 Woody Hayes Drive, Columbus, OH 43210, USA
* Correspondence: huang.6338@osu.edu

Abstract

The global transition towards sustainable food systems has intensified the search for alternative protein sources that can meet human nutritional demands with reduced environmental impacts. Although microalgae are rich in protein, their applications in food remain limited due to thick cell walls and intense green color. The aim of this study is to modify *Chlorella vulgaris* by high-pressure homogenization (HPH) and decolorization to improve its processability for extrusion-based 3D printing. Microalgal biomass was pretreated by HPH at different pressures (10,000, 15,000, 20,000 psi) for one to three passes, followed by pigment removal using ethanol of different concentrations (70, 85, 100%). Microscopic imaging shows that HPH effectively disrupted microalgal cell walls and caused cell disintegration, resulting in increased foaming stability (22–28%) but lower solubility (up to 24%), with other functional properties largely preserved. Ethanol treatments markedly decolored microalgae and increased their water-holding capacity (10–45%) and solubility (6–11%). The formulation of HPH-treated decolorized microalgae with soy protein isolate and xanthan gum increased the viscosity (66–179%) and elasticity (78–235%) of printing inks. The resulting 3D prints show higher hardness (47–128%), springiness (up to 155%) and chewiness (47–408%). The information obtained from this study provides guidance for modifying the functional and rheological properties of microalgae and contributes to advancing the formulation and manufacturing of microalgae-based foods.

Keywords: algae; chlorophyll; texture profile; elastic module; bioaccessibility; emulsifying properties

Check for updates

Academic Editors: Giannis Penloglou and Alexandros Pavlou

Received: 26 February 2026
Revised: 1 April 2026
Accepted: 7 April 2026
Published: 10 April 2026

Copyright: © 2026 by the authors. Licensee MDPI, Basel, Switzerland. This article is an open access article distributed under the terms and conditions of the Creative Commons Attribution (CC BY) license.

1. Introduction

Microalgae are a nutrient-rich biomass with high light conversion efficiency (8–10%), making them a sustainable source of ingredient and food [1]. For example, species within the *Chlorella* genus, such as *Chlorella vulgaris*, have high protein contents (approximately 40–60%) and balanced amino acid profiles, and several have been classified as "GRAS" (Generally Recognized as Safe) by the FDA for use as an ingredient in certain foods [2]. These characteristics position *Chlorella* as a promising alternative protein source for innovative plant-based food formulations [3]. However, *Chlorella*'s applications in foods

remain limited owing to several intrinsic factors. First, *Chlorella* has a rigid chitin-like cell wall, impeding protein digestibility and bioaccessibility [4,5]. One of the others is its dark green pigmentation and characteristic odors, which negatively affect their sensory acceptance. These features hinder *Chlorella*'s incorporation into visually appealing or delicately flavored products.

Additive manufacturing, particularly extrusion-based 3D food printing, has emerged as an innovative technology for designing customizable, nutritionally targeted, and structurally complex foods [6]. The formulation of the printable "inks" is critical. They must possess suitable functional and rheological properties to enable smooth extrusion and stable shape retention [7]. Previous studies have incorporated 1–20% (*w*/*w*) microalgae (*Chlorella* and *Spirulina*) into 3D-printing formulations, as summarized by Mirzapour-Kouhdasht et al. (2024) [8]. However, formulations with intact microalgal cells still present challenges due to the rigid cell walls, which restrict both their functional performance in inks and protein digestibility of the final printed products.

The microalgal cell can be disrupted by several techniques [9], among which mechanical methods, such as high-pressure homogenization (HPH), have gained particular interest because of its efficiency, controllability, and ability to preserve nutritional components [10,11]. When treating microalgae with HPH, the intense turbulence, shear, impingement, and cavitation generated can rupture their cell walls to facilitate the release of intracellular components, thereby improving the extractability, solubility, and digestibility of target nutrients [12]. HPH can also induce controlled microstructural modifications in microalgal biomass that enhance functional properties, hydration capacity, emulsification, and viscoelastic behavior [13]. Furthermore, HPH produces finer dispersions with better uniformity, which, when incorporated into food formulations, can improve the structural recovery of the materials.

Pigment reduction in microalgae is often necessary to increase their sensory acceptability for food applications and is commonly achieved by solvent extraction methods. Aqueous methanol, ethanol and acetone solutions are widely employed for extraction of microalgal pigments [14]. Ethanol-based extraction of chlorophyll has been shown to effectively lighten *Chlorella* biomass while maintaining its nutritional value [15].

Although HPH and solvent extraction can improve the nutrient bioaccessibility and visual appeal of microalgae for human consumption, respectively, their combined effects on the processability of microalgae-based food materials are still unclear. For example, for extrusion-based 3D printing, material (ink) rheology is especially critical, as printable inks must flow smoothly through the nozzle and rapidly recover their structural integrity after deposition [16]. However, no studies, to the best of the authors' knowledge, have been performed to systematically evaluate the effects of HPH and pigment reduction on the printability of microalgae-based 3D printing inks.

In this study, HPH operated at different pressures and numbers of passes and solvent extraction performed in different ethanol–water ratios were applied as pretreatments on *C. vulgaris* biomass for cell wall disruption and chlorophyll removal, respectively, and the functionalities of pretreated microalgae were analyzed. Additionally, the rheology of food printing inks containing pretreated microalgae as well as the texture and protein bioaccessibility of resulting extrusion-based 3D prints were comprehensively studied. These evaluations aim to identify pretreatment conditions that can increase the addition of microalgae into printing inks, without compromising, or even improving, their printability and nutritional integrity.

2. Materials and Methods

2.1. Materials

C. vulgaris powder (XPRS Nutra, Las Vegas, NV, USA; purchased through Amazon.com), soy protein isolate (SPI; Skidmore Sales and Distribution, Saratoga Springs, NY, USA), and xanthan gum (Hznxolrc, Arlington, VA, USA) were used for printing ink formulation. All the chemicals, including sodium dodecyl sulfate (SDS), 2,4-dinitrophenylhydrazine (DNPH), trichloroacetic acid (TCA), and ethanol, were of analytical grade and purchased from Fisher Scientific (Waltham, MA, USA).

2.2. HPH Treatment

C. vulgaris powder was dispersed in distilled water in a ratio of 1:10 (*w*/*v*) and pre-homogenized at 4000 rpm for 4 min using a high-shear disperser (ULTRA-TURRAX T25, IKA Works Inc., Wilmington, NC, USA) to ensure uniform dispersion. The dispersion was then passed through a high-pressure homogenizer (PandaPLUS 2000, GEA Niro Soavi, Parma, Italy) for treatment at different pressure levels (10,000, 15,000, and 20,000 psi, equivalent to 69, 103, and 138 MPa, respectively) for different numbers of passes (one, two, and three). The sample temperature was monitored and controlled at <50 °C during HPH using a circulating water bath integrated in the PandaPLUS system, which was kept at 3 °C. All the samples were frozen at −20 °C immediately after HPH, then freeze-dried (Harvest Right, North Salt Lake City, UT, USA) to ensure minimal effects on the sample properties to be analyzed. The freeze-dried sample was ground using an Electric Grain Mill Grinder (Samger, Shenzhen, China) at 28,000 rpm for 1 min to obtain homogeneous powder. The resulting sample was stored in a sealed, airtight container at room temperature until further analysis. The control sample prepared by dispersing *C. vulgaris* powder dispersed in distilled water but without HPH treatment before freeze-drying and grinding, following the identical steps described above, was used as the control in this study, unless otherwise stated.

2.3. Chlorophyll Removal

Chlorophyll removal from HPH-treated microalgae was performed through a series of ethanol washing. Following the steps described in the previous section, *C. vulgaris* powder was first homogenized at 20,000 psi for one pass, the condition considered as optimal according to the results of microalgal functionality, printing ink rheology and 3D print texture reported in Sections 3.1–3.5. After HPH, the sample was centrifuged (Multifuge X4 Pro Centrifuge, Thermo Fisher Scientific, Waltham, MA, USA) at 12,000× *g* and 4 °C for 10 min to pellet the disrupted biomass.

Ethanol solutions in three concentrations, 70, 85, and 100% (*v*/*v*), were used for chlorophyll removal. For each concentration, three sequential ethanol washes were performed. During each wash, the pellet of microalgal biomass was resuspended in the ethanol solution by vortexing for 10 s, followed by agitation using an orbital shaker for 10 min at room temperature. After agitation, the sample was centrifuged at 12,000× *g* for 10 min under 4 °C to collect the pellet. The same volume of fresh ethanol solution was added to the pellet for the next wash. The same procedure was repeated three times for each chlorophyll removal treatment.

After decolorization, the microalgal biomass pellet was washed with deionized water three times to remove residual ethanol then placed in a desiccator overnight before freeze-drying. The dried sample was ground and the resulting powder was stored at room temperature until further analysis.

The color of the decolorized microalgal biomass was measured using a HunterLab LabScan XE colorimeter (Hunter Associates Laboratory Inc., Reston, VA, USA) and presented by the CIE L^* (lightness), a^* (red/green), and b^* (yellow/blue) values.

2.4. Morphology and Functional Property Analyses on Microalgae

2.4.1. Microscopic Imaging

Microalgae powder suspensions were visualized using a light microscope (BX43; Olympus, Tokyo, Japan) equipped with a dual charged-coupled device camera (DP80; Olympus, Tokyo, Japan) to identify changes in particle dispersion and appearance caused by different HPH treatments. Images were taken under consistent lighting and background conditions to ensure comparability among samples.

2.4.2. Water-Holding Capacity (WHC) and Solubility

The WHC of microalgae was quantified following the method described by Beuchat [17] with slight modifications. Approximately 0.5 g of the freeze-dried, HPH-treated microalgae powder (referred to as microalgae powder hereinafter) with or without decolorization was dispersed in 10 mL of distilled water, vortexed, and centrifuged at 5000× g for 20 min. The supernatant was decanted, and the amount of water retained was calculated by the weight difference between the hydrated (W_{wet}) and dry (W_{dry}) samples.

$$\text{WHC}(\text{g/g}) = \frac{W_{wet} - W_{dry}}{W_{dry}} \quad (1)$$

The solubility of microalgae was determined using the supernatant collected. Aliquot was dried at 100 °C for 24 h and the solid dry residue was weighed. The solubility (%) was calculated as the weight ratio of dried soluble solids (W_{soluble}) to the initial dried powder (W_{initial}).

$$\text{Solubility}(\%) = \left(\frac{W_{soluble}}{W_{initial}}\right) \times 100 \quad (2)$$

2.4.3. Emulsifying Activity Index (EAI) and Emulsion Stability Index (ESI)

The emulsifying properties of microalgae were determined following the method of Pearce and Kinsella (1978) [18] with modifications. A 0.5% (w/v) dispersion was prepared by dispersing 0.15 g of microalgae powder into 30 mL of deionized water. Then, 30 mL of the dispersion was homogenized with 10 mL of canola oil (oil-to-aqueous ratio 1:3, oil volume fraction ϕ = 0.25) using an IKA T50 Ultra-Turrax homogenizer (IKA Works, Wilmington, NC, USA) at 10,000 rpm for 2 min to form an emulsion. Fifty microliters of the emulsion were diluted by 5 mL of 0.1% (w/v) SDS to ensure complete droplet dispersion. The absorbance of the diluted sample was measured at 500 nm using a Genesys 30 Visible Spectrophotometer (Thermo Scientific, Waltham, MA, USA) at 0 min (immediately after dilution, A_0) and 10 min (A_{10}).

$$\text{EAI}(\text{m}^2/\text{g}) = \left(\frac{2 \times T \times A_0 \times 2.303}{C \times \phi}\right) \times 100 \quad (3)$$

where the leading coefficient 2 accounts for the optical path length factor resulting from light scattering which occurs in both forward and backward directions, T is the dilution factor (i.e., 100), 2.303 is the conversion factor from absorbance to turbidity, and C is the protein concentration of the aqueous phase (g/mL) calculated based on the protein content of microalgae (64.4%), which was determined using the bicinchoninic acid (BCA) assay (Smith et al., 1985) [19].

The ESI was determined by:

$$\mathrm{ESI(min)} = \left(\frac{A_0}{A_0 - A_{10}}\right) \times 10 \quad (4)$$

where 10 represents the time interval (min) between the two absorbance readings.

2.4.4. Foaming Capacity (FC) and Foam Stability (FS)

The foaming property of microalgae was determined following Mirzapour-Kouhdasht et al. (2021) [20] with slight modifications. Briefly, a 2% (*w*/*v*) dispersion was prepared with microalgae powder by whipping at 10,000 rpm for 2 min using the IKA T50 Ultra-Turrax homogenizer. The volume of foamed dispersion was recorded immediately (V_0) and after 30 min (V_{30}) to calculate FC and FS using the following equations:

$$\mathrm{FC(\%)} = \left(\frac{V_0 - V_{initial}}{V_{initial}}\right) \times 100 \quad (5)$$

where V_{initial} is the volume of the dispersion before homogenization.

$$\mathrm{FS(\%)} = \left(\frac{V_{30}}{V_0}\right) \times 100 \quad (6)$$

2.5. 3D Printing Ink Preparation and Characterization

Microalgae-based ink was formulated by mixing microalgae powder (19.4% in weight), either decolorized or non-decolorized, with SPI (13.0%) and distilled water (67.1%). Xanthan gum (0.5%) was added to improve printability and structural stability [21,22]. The dry ingredients were gradually added into the water under manual stirring until a uniform mixture was formed.

The rheological properties of ink were analyzed following Habib and Khoda (2022) [23] with modifications. A controlled stress rheometer (DHR-3, TA Instruments, New Castle, DE, USA) equipped with 40 mm parallel plate and a fixed gap of 1000 µm was used for the analysis. The sample was carefully loaded to avoid structural disruption before testing. The linear viscoelastic region (LVR) of the ink was determined by conducting an oscillation amplitude sweep at an angular frequency of 3 rad/s. The test strain was set to increase logarithmically from 0.01% to 100% at 20 °C after a 90 s equilibration period. The storage modulus (G′) and loss factor (tan δ) were measured to characterize the elastic and viscous behaviors of the ink. The apparent viscosity of the ink was determined using a flow sweep with a shar rate ranging from 0.1 to 100 s^{-1} at 25 °C after a 180 s soak period.

2.6. 3D Printing and Post-Printing Analysis

3D printing of microalgae-based ink was carried out using a Foodini printer (Natural Machines, Barcelona, Spain) equipped with a 0.8 mm nozzle. Key printing parameters, including a printing speed of 10 mm/s, an ingredient flow factor of 1.35, and a 20% infill density, were set within the manufacturer's recommended range and further adjusted through preliminary trials to ensure continuous and uniform extrusion, stable filament deposition, and reproducible print quality. The sample was printed as a 2 × 2 × 2 cm cube for the following texture profile analysis (TPA).

TPA of the 3D print was conducted using a TA.XT2i Texture Analyzer (Stable Micro Systems, Surrey, UK) equipped with a 40 mm cylindrical probe (P/40) and a 5 kg load cell. A double-compression test to 25% deformation was performed following typical protocols used for 3D-printed foods [24,25], at pre-test and test speeds both of 1 mm/s and a post-test speed of 10 mm/s, with a 30 s interval between compressions to allow partial structural

recovery. Textural attributes, including hardness, adhesiveness, cohesiveness, resilience, springiness, and chewiness, were computed using the Exponent Connect software version 7.0 (Stable Micro Systems, Surrey, UK).

To evaluate the protein bioaccessibility of the print, in vitro digestion was performed following the standardized INFOGEST static protocol [26] with slight modifications. Briefly, a sample of 5 g dry weight was mixed with 3.5 mL of simulated salivary fluid containing 0.3 M calcium chloride (0.025 mL) and α-amylase (0.5 mL, 1500 U/mL), adjusted to the protocol-specified conditions, and incubated at 37 °C for 2 h, then the reaction was stopped by heating at 95 °C for 10 min. The resulting oral bolus was combined with simulated gastric fluid, pepsin, $CaCl_2$, and acid to reach the required INFOGEST gastric conditions, followed by incubation at 37 °C for 2 h and enzyme inactivation by boiling for 10 min. The gastric chyme was then mixed with simulated intestinal fluid, pancreatin, bile salts, $CaCl_2$, and sodium hydroxide according to the INFOGEST formulation, incubated again at 37 °C for 2 h, and finally heat-treated at 95 °C for 10 min to stop intestinal digestion. After digestion, the sample was centrifuged to obtain the soluble fraction. Protein concentration was quantified using the BCA assay for the initial undigested sample and the intestinal supernatant. Protein bioaccessibility (%) was calculated as the ratio of soluble intestinal-phase protein to the initial protein content of the print.

2.7. Statistical Analysis

All the experiments were carried out in triplicate. Results are presented as mean ± standard deviation. One-way ANOVA was performed to determine significant differences among treatments, and Tukey's HSD test was applied for pairwise comparisons ($p < 0.05$). Statistical analysis was performed using the JMP Pro 19 software (SAS Institute Inc., Cary, NC, USA) and graphical outputs were generated using the GraphPad Prism software version 10.6.1 (GraphPad Software, San Diego, CA, USA).

3. Results and Discussion

3.1. Microscopic Imaging of HPH-Treated Microalgae

Figure 1 shows the images of microalgae before and after HPH treatments. The control displayed intact, spherical cells in the size of ~7 µm with clear cell walls. All the HPH-treated microalgae showed visible cell rupture, which became clearer as the pressure and/or number of passes increased. At 10,000 psi, especially after one pass, most cells remained intact with few ruptured ones. After three passes, cell integrity visibly declined owing to repeated exposure to mechanical stresses. At 15,000 psi, only small cells were observed after one pass and more passes resulted in much more pronounced rupture with nearly no cell walls shown. Treatments at 20,000 psi basically caused complete structural disintegration, even after one pass, with only isolated fragments and intracellular components observed, demonstrating that this level of pressure surpassed the structural resistance of the microalgal cell wall. These observations align with the literature which shows that pressures ≥ 15,000 psi are typically needed to disrupt *Chlorella* cells due to their rigid wall composition [12].

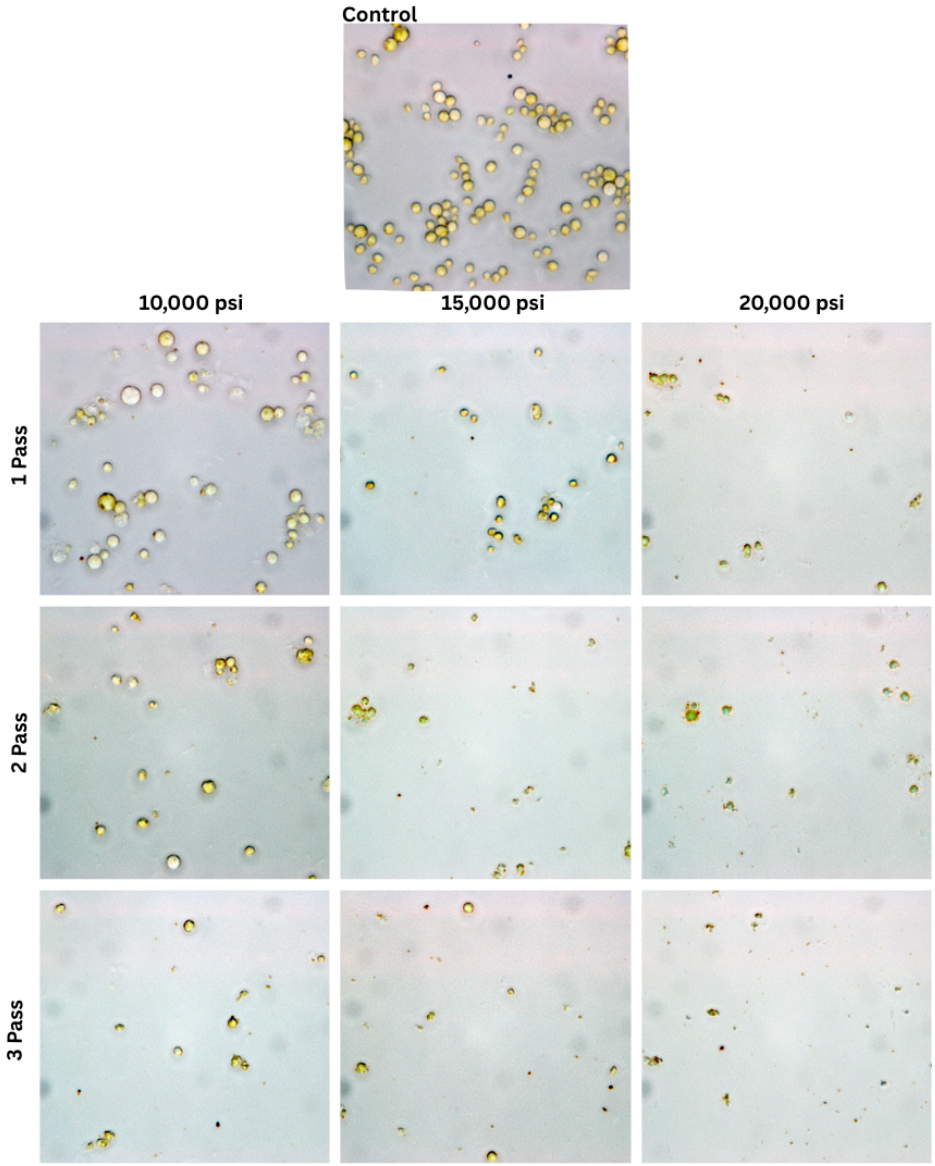


Figure 1. Microscopic images (100× magnification) of *C. vulgaris* treated with high-pressure homogenization at different pressures for different numbers of passes.

3.2. Functional Properties of HPH-Treated Microalgae

HPH treatments generally reduced the solubility of microalgae by up to 24%, as shown in Table 1, although the effects of pressure and number of passes were not significant. The reduction suggests that although HPH can disrupt the rigid microalgal cell wall and release intracellular proteins into the aqueous phase, the conditions tested in this study generated mechanical stresses that could be intense enough to induce protein aggregation or partial denaturation and thus limit the solubility. Similar findings have been reported for microalgal proteins processed by high shear, which resulted in protein unfolding and exposure of hydrophobic residues, promoting intermolecular association [27]. It is important to note that the most intense HPH treatment condition, i.e., 20,000 psi for three passes, made microalgae have a significantly higher solubility (73.08%) than the other treated samples. This could be because this level of treatment caused more extensive cell fragmentation and released other intracellular components such as polysaccharides, cell wall fragments, pigments, lipids and small metabolites, which may counterbalance the effect of protein aggregation.

Table 1. Functional properties of *C. vulgaris* powder treated by high-pressure homogenization at 10,000, 15,000, and 20,000 psi for 1, 2, and 3 passes.

Pressure (psi)	Passes	Solubility (%)	WHC (g/g)	EAI (%)	ESI (%)	FC (%)	FS (%)
Control	0	74.13 ± 2.98 ^{a}	1.19 ± 0.03 ^{a}	5.64 ± 0.45 ^{a}	26.39 ± 4.79 ^{a}	31.00 ± 1.41 ^{a}	76.13 ± 6.09 ^{b}
10,000	1	64.82 ± 2.95 ^{abc}	1.21 ± 0.02 ^{a}	5.34 ± 0.72 ^{a}	27.52 ± 2.42 ^{a}	24.00 ± 5.66 ^{a}	95.67 ± 2.89 ^{a}
10,000	2	65.71 ± 6.06 ^{abc}	1.15 ± 0.03 ^{ab}	5.81 ± 0.14 ^{a}	25.12 ± 2.18 ^{a}	32.00 ± 3.00 ^{a}	97.23 ± 2.33 ^{a}
10,000	3	56.26 ± 2.61 ^{c}	1.05 ± 0.02 ^{bcd}	5.53 ± 0.34 ^{a}	32.91 ± 1.75 ^{a}	29.33 ± 0.58 ^{a}	93.03 ± 5.83 ^{a}
15,000	1	64.15 ± 1.74 ^{bc}	1.05 ± 0.04 ^{bcd}	5.23 ± 0.89 ^{a}	26.05 ± 5.58 ^{a}	31.33 ± 2.89 ^{a}	93.60 ± 4.31 ^{a}
15,000	2	59.35 ± 3.74 ^{c}	1.00 ± 0.02 ^{cd}	6.09 ± 0.81 ^{a}	35.56 ± 6.11 ^{a}	31.00 ± 1.00 ^{a}	93.00 ± 4.36 ^{a}
15,000	3	60.14 ± 2.74 ^{c}	0.95 ± 0.09 ^{d}	5.67 ± 0.11 ^{a}	27.76 ± 3.44 ^{a}	31.00 ± 6.56 ^{a}	92.77 ± 5.70 ^{a}
20,000	1	58.59 ± 3.53 ^{c}	1.16 ± 0.05 ^{ab}	6.46 ± 0.54 ^{a}	30.00 ± 6.21 ^{a}	30.33 ± 6.03 ^{a}	98.47 ± 0.70 ^{a}
20,000	2	57.16 ± 1.54 ^{c}	1.11 ± 0.04 ^{abc}	5.91 ± 0.78 ^{a}	35.91 ± 10.12 ^{a}	31.33 ± 4.51 ^{a}	95.63 ± 2.37 ^{a}
20,000	3	73.08 ± 0.58 ^{ab}	1.11 ± 0.05 ^{abd}	6.61 ± 0.53 ^{a}	28.50 ± 6.09 ^{a}	30.33 ± 3.21 ^{a}	97.20 ± 2.44 ^{a}

Values are expressed as mean ± standard deviation of triplicate. Different superscript letters within a column indicate significant differences ($p < 0.05$). WHC: water-holding capacity; EAI: emulsifying activity index; ESI: emulsion stability index; FC: foaming capacity; FS: foaming stability.

Compared to solubility, the WHC of microalgae remained relatively unchanged after HPH treatments; only the samples treated at 15,000 psi showed significantly reduced values, by 17–20% (Table 1). The HPH treatments applied in this study had no significant effect on the EAI and ESI of microalgae. Similar results were reported in the study of Folgado et al. (2026) [28] on algae oil microencapsulation—that the homogenization technique did not influence emulsion stability. In contrast, Ebert et al. (2019) [29] indicate that HPH can increase the surface activity of microalgal proteins and improve their interfacial behavior, and Georgiou et al. (2024) [30] also reported that microalgal cell disruption can enhance emulsion stability through both protein-driven interfacial film formation and particle-assisted stabilization.

The FC of microalgae did not significantly change after HPH treatments. Although HPH can facilitate the release of intracellular proteins, Georgiou et al. (2024) [30] observed that the FC of microalgal dispersions changed only marginally, indicating that cell disruption alone is insufficient to obtain highly foaming *Chlorella* ingredients and additional protein fractionation or formulation treatments are needed. In contrast, the FS of microalgae was improved dramatically by HPH for all the cases, by 22–28%, although the pressure and number of passes did not have significant effects. This improvement reflects the formation of stronger, more elastic interfacial protein films resulting from partial unfolding of proteins. Disrupted cell fragments may further contribute to FS by reinforcing bubble walls through Pickering-like stabilization mechanism [31]. This result corresponds to Katsimichas et al. (2024) [27] who found that HPH enhanced the stability of foams formed by microalgal and marine proteins by improving their interfacial viscoelasticity.

3.3. Rheological Analysis on Printing Inks Containing HPH-Treated Microalgae

All the inks containing microalgae, regardless of HPH treatment, exhibited the same shear-thinning behavior, as shown in Figure 2. The ink viscosity varied noticeably with HPH intensity, particularly at a shear rate < 1/s. Increasing the pressure from 10,000 (Figure 2a) to 15,000 (Figure 2b) psi considerably increased the ink viscosity, regardless of the number of passes. Further increase in pressure to 20,000 psi hardly affected the viscosity (Figure 2c), except for the one-pass treatment. At 10,000 and 15,000 psi, treating microalgae for the second pass increased the ink viscosity, but adding one more pass did not have a significant effect. The effect of number of passes on the viscosity was negligible for treatments at 20,000 psi. The increase in viscosity can be attributed to the intracellular

proteins and polysaccharides released with microalgal cell disruption, which can thicken the continuous phase [27,32].

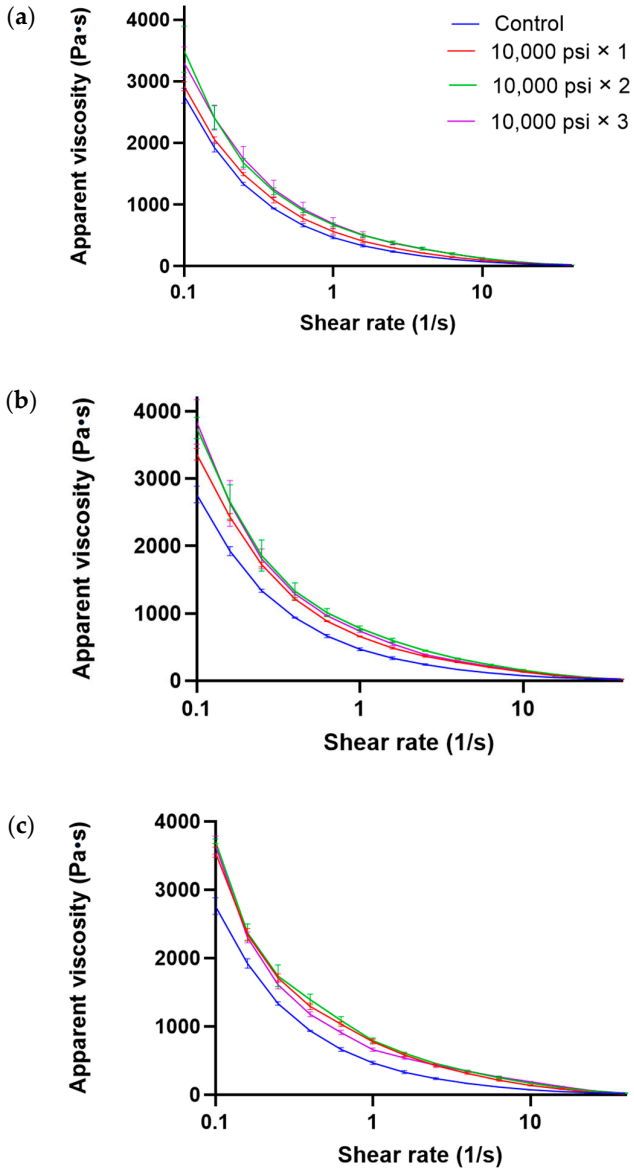


Figure 2. Apparent viscosity of 3D printing inks formulated with *C. vulgaris* treated by high-pressure homogenization at (**a**) 10,000, (**b**) 15,000, and (**c**) 20,000 psi for different numbers of passes (1, 2 and 3).

HPH treatments on microalgae increased the G′ of the inks prepared (Figure 3) by 3–47%, except for the case of 10,000 psi for one pass, consistent with the findings of Magpusao et al. (2021) [13]. In general, increasing the HPH intensity (higher pressure and/or more passes) resulted in higher G′. The increased G′ can be due to the proteins and polysaccharides released along with microalgal cell disruption which interact with SPI and xanthan gum in the ink to strengthen the network formed [27,33]. However, extreme HPH conditions can induce protein aggregation [34], which may explain the lower G′ observed for the 20,000 psi, three-pass treatment than that for the 20,000 psi, two-pass one.

As shown in Figure 4, the tan δ of all the inks remained below 1 within the LVR (5–10% strain), indicating the characteristics of viscoelastic gel rather than liquid [35]. HPH treatments on microalgae, regardless of the condition, slightly increased the tan δ of the resulting inks by 6–34%, implying that HPH caused a larger rise in G″ than in G′. Furthermore, the tan δ became higher as the HPH intensity increased. When the strain

applied exceeded 10%, the tan δ became larger than 1 for all the inks. For the microalgae treated at 10,000 and 15,000 psi (Figure 4a,b), the resulting inks had lower tan δ than the control, indicating that once the structural network formed in the ink started to yield, HPH-treated microalgae allowed the ink to retain a more elastic response. In contrast, in the case of 20,000 psi (Figure 4c), HPH treatments increased the tan δ, suggesting that severe homogenization made the gels formed become more viscous at elevated strains. Similar behavior was observed for *Chlorella*-pea gels—that excessive HPH may weaken the elastic gel network instead of strengthening it [13].

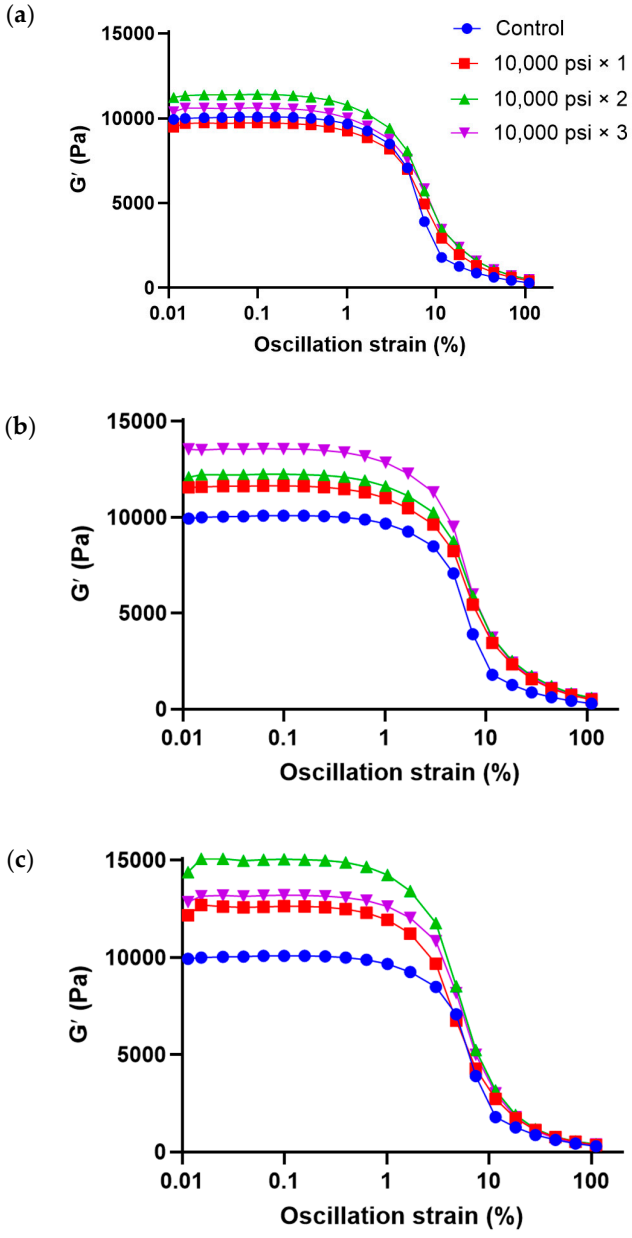


Figure 3. Storage modulus (G′) of 3D printing inks formulated with *C. vulgaris* treated by high-pressure homogenization at (**a**) 10,000, (**b**) 15,000, and (**c**) 20,000 psi for different numbers of passes (1, 2 and 3).

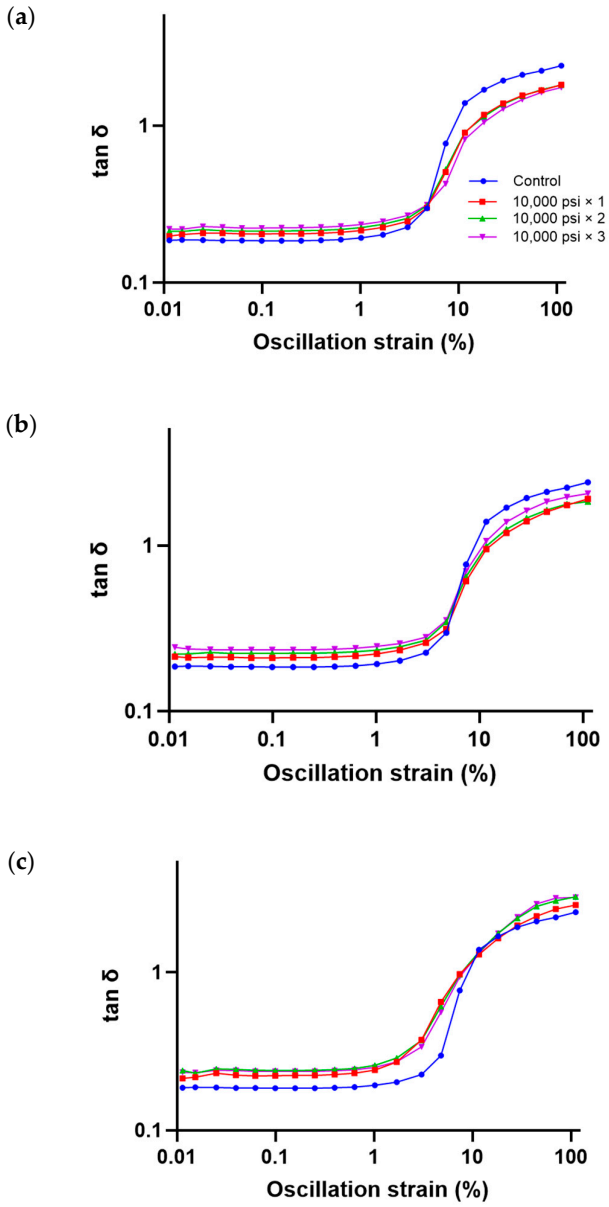


Figure 4. Loss factor (tan δ) of 3D printing inks formulated with *C. vulgaris* treated by high-pressure homogenization at (**a**) 10,000, (**b**) 15,000, and (**c**) 20,000 psi for different numbers of passes (1, 2 and 3).

3.4. Texture Profiles of Microalgae-Based 3D Prints

Although incorporating HPH-treated microalgae increased the G′ of the inks (Figure 3), all the inks remained extrudable due to their high water content (~67%). Figure 5 shows that HPH-treated microalgae altered the texture profiles of the resulting 3D prints by decreasing the adhesiveness (25–73%), cohesiveness (13–25%) and chewiness (5–36%) and increasing the resilience (17–55%). Increasing the HPH pressure or number of passes generally decreased the adhesiveness, cohesiveness and chewiness, although the trends became less significant as the treatment intensity increased. In contrast, the effect HPH intensity on the resilience was relatively limited, if not negligible.

The increased G′ of microalgae-based inks did not necessarily translate into harder macroscopic structures after printing. This could be attributed to more fine microalgae debris generated after more intense HPH (Figure 1), leading to formation of less particulate-reinforced networks. Moreover, the intensities of the HPH treatments applied in this study could promote protein aggregation and thus make the networks more brittle. Mosibo et al. (2024) [36] also found that excessive homogenization reduced the firmness of gels

formed by plant-based proteins and microalgae by eliminating larger structural elements and increasing water mobility in the gels.

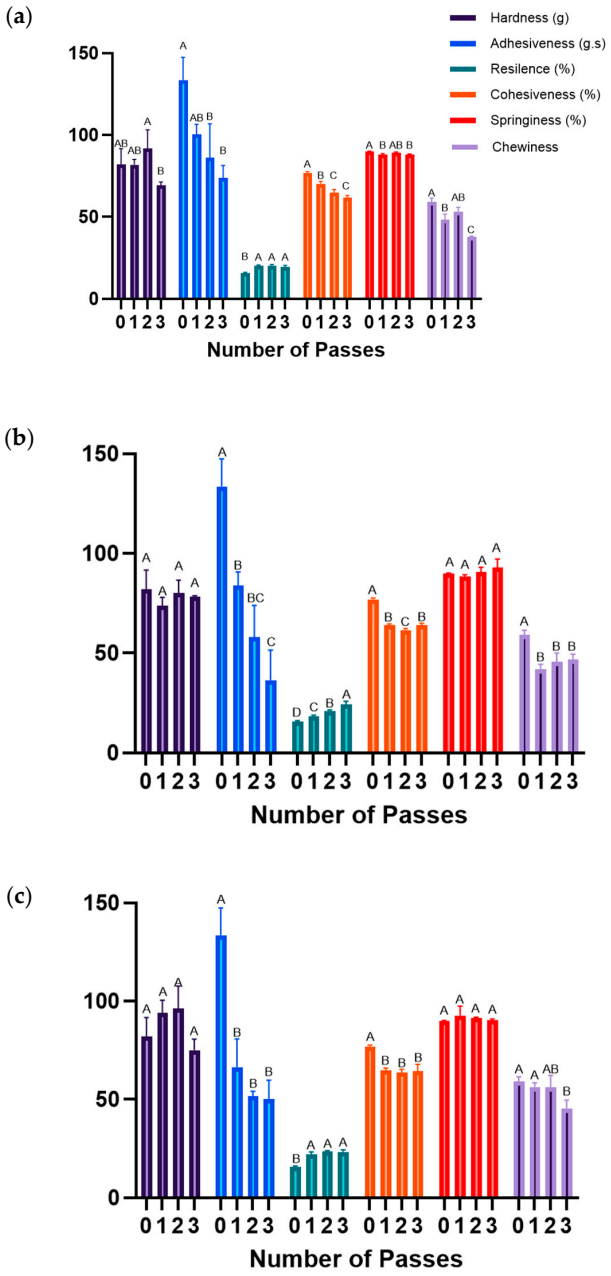


Figure 5. Hardness (g), adhesiveness (g s), resilience (%), cohesiveness (%), springiness (%) and chewiness of 3D prints from inks formulated with *C. vulgaris* homogenized at (**a**) 10,000, (**b**) 15,000, and (**c**) 20,000 psi for different numbers of passes (1, 2 and 3). Different letters within the same color group indicate significant difference among the values ($p < 0.05$).

3.5. Protein Bioaccessibility of 3D Prints

Table 2 shows the effect of HPH-treated microalgae on the protein bioaccessibility of the print. The treatments at 10,000 psi or for one pass did not significantly affect the bioaccessibility, but those at 15,000 and 20,000 psi for two to three passes resulted in significant decreases, by 16–24%. These results are opposite to the expectation that HPH would enhance protein accessibility due to the disruption of the rigid polysaccharide-rich cell wall of microalgae, which is widely considered as a major barrier to nutrient accessibility [12]. While Rahman et al. (2022) [37] report that physical disruption of the microalgal cell wall

improved the accessibility of intracellular components, one possible explanation for our findings is the formation of protein aggregates during intense homogenization, particularly under high pressure and multiple passes. Such aggregation can reduce the solubility (Table 1) and thus enzymatic accessibility of proteins [38]. Additionally, high mechanical stress might induce conformational changes or cross-linking, rendering proteins less susceptible to proteolytic enzymes such as pepsin and pancreatin used in the INFOGEST protocol. It is also important to note that microalgae contain other components, such as polyphenols, fiber, and chlorophyll, which can be released after HPH and may interact with proteins and digestive enzymes, thereby reducing digestion efficiency and further inhibiting protein bioaccessibility [3]. The results suggest that mild or moderate treatment conditions could be better options for balancing cell disruption with protein bioaccessibility.

Table 2. Protein bioaccessibility of 3D prints containing *C. vulgaris* treated by high-pressure homogenization at different pressures for different numbers of passes.

Pressure (psi)	Passes	Protein Bioaccessibility (%)
Control	0	16.07 ± 0.61^{a}
10,000	1	14.11 ± 0.64^{abc}
10,000	2	14.08 ± 1.41^{abc}
10,000	3	14.91 ± 1.22^{ab}
15,000	1	14.07 ± 0.56^{abc}
15,000	2	13.42 ± 0.11^{bc}
15,000	3	13.03 ± 0.23^{bc}
20,000	1	14.13 ± 0.94^{abc}
20,000	2	13.13 ± 1.36^{bc}
20,000	3	12.21 ± 0.25^{c}

Values represent mean ± standard deviation. Different superscript letters indicate significant difference among the values ($p < 0.05$).

3.6. Effects of Chlorophyl Removal

3.6.1. Decolorization of HPH-Treated Microalgae

The selected HPH-treated microalgae (20,000 psi for one pass) were washed by ethanol solutions of different concentrations for decolorization, as described in Section 2.3. Ethanol washing caused a clear change in the color of *C. vulgaris*, as shown by the shifts in L^*, a^*, and b^* values (Table 3). The L^* value significantly increased by 25, 29 and 35, after the 70%, 85%, and 100% ethanol treatments, respectively. The a^* value significantly increased by 4.7, 4.2 and 2.8 with increasing ethanol concentration. These increases indicate that the microalgae became markedly lighter with reduced greenness, due to pigment, especially chlorophyll, removal. The b^* value also significantly increased by 18 (70% ethanol), 16 (85%) and 12 (100%), reflecting a shift toward more yellow tones because other cellular components became more visible when chlorophyll was removed. It is important to note that the 75% ethanol treatment resulted in larger changes in the a^* and b^* values although it was less impactful on the L^* value.

Table 3. Color parameters of high-pressure homogenized (20,000 psi for one pass) *C. vulgaris* washed by ethanol solutions of different concentrations.

Ethanol Concentration (%)	L^*	a^*	b^*
Unwashed	21.27 ± 0.14^{D}	3.24 ± 0.04^{A}	13.13 ± 0.19^{D}
70	46.48 ± 0.04^{C}	7.97 ± 1.01^{D}	31.23 ± 0.02^{A}
85	50.67 ± 0.02^{B}	7.39 ± 0.02^{C}	29.39 ± 0.01^{B}
100	56.57 ± 0.09^{A}	6.00 ± 0.01^{B}	25.61 ± 0.03^{C}

Values are expressed as mean ± standard deviation of triplicate. Different superscript letters within a column indicate significant differences ($p < 0.05$).

3.6.2. Functional Properties of HPH-Treated Decolorized Microalgae

Chlorophyl removal by ethanol treatment had different effects on the functional properties of microalgae, as shown in Figure 6. Both the WHC (Figure 6a) and solubility (Figure 6b) increased significantly by 10–45% and 6–11%, respectively, and the treatment of 100% ethanol resulted in the highest WHC. These can be attributed to removal of hydrophobic pigments which improved the ability of microalgae to retain water without notably disrupting the protein matrix. Similar findings have been reported—that partial removal of non-protein components can enhance the solubility and functionality of microalgal and soy proteins [39,40]. Ethanol treatments markedly changed the emulsifying properties of microalgae, and the concentration had significant effects. The EAI decreased sharply with increasing ethanol concentration, by 18–90% (Figure 6c), which is in line with Feng et al. (2021) [41] because ethanol altered the surface hydrophobicity of microalgae and reduced their ability to adsorb and stabilize newly formed oil–water interfaces. Despite significant differences from the unwashed sample by up to 305% (85% ethanol treatment; Figure 6d), the ESI of decolorized microalgae did not show a consistent trend and the reason is unclear. The foams formed by decolorized microalgae were more persistent, with 8–19% higher FS (Figure 6f, although their FC were not significantly altered (Figure 6e, except the sample treated with 70% ethanol which had a considerably lower FC than the unwashed one.

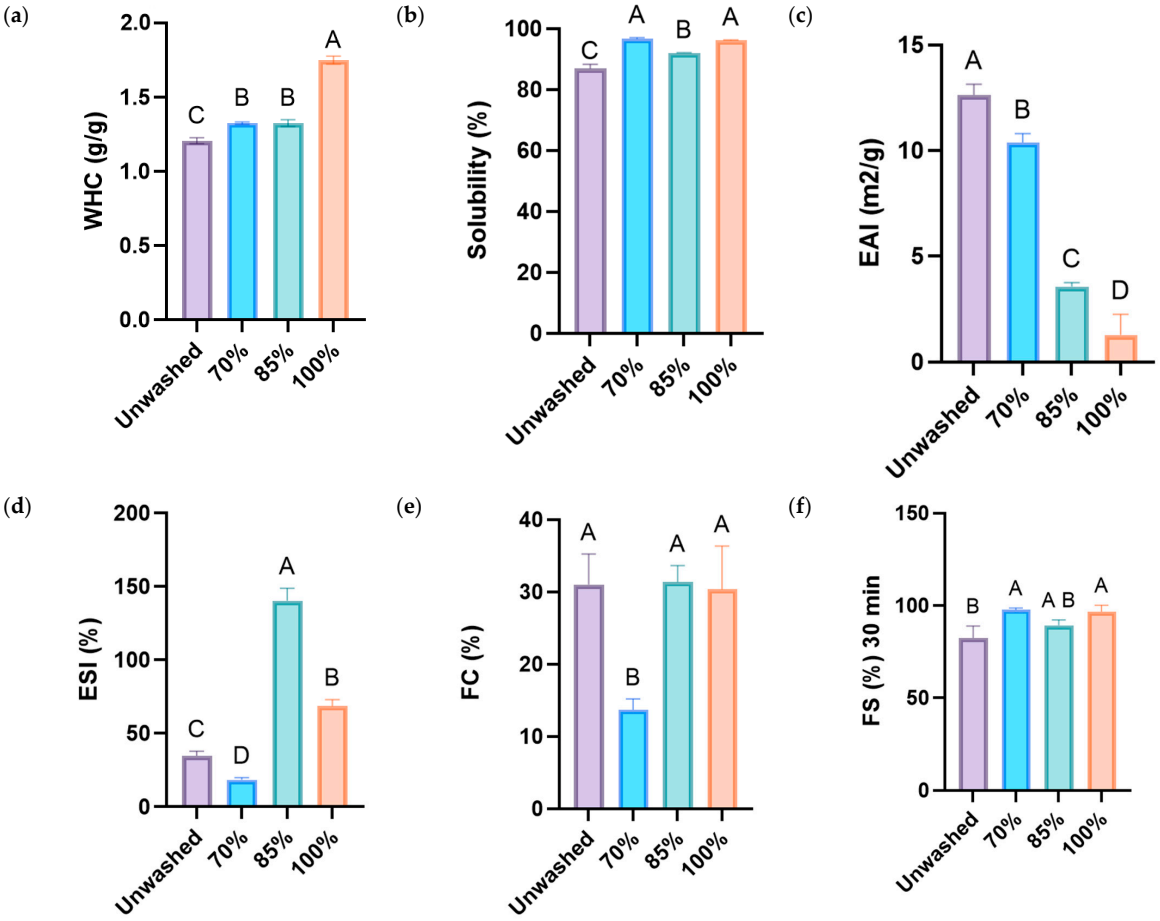


Figure 6. (**a**) Water-holding capacity, (**b**) solubility, (**c**) emulsifying activity index, (**d**) emulsifying stability index, (**e**) foaming capacity, and (**f**) foaming stability of high-pressure homogenized (20,000 psi for one pass) *C. vulgaris* decolorized by ethanol solutions of different concentrations. Bars indicated with different letters have significantly different values ($p < 0.05$).

3.6.3. Rheological Properties of Printing Inks Containing HPH-Treated Decolorized Microalgae

Because the inks formulated with microalgae treated by 85% and 100% ethanol were too rigid for printing, 15% more water was added to the ink formulation to ensure that all the inks prepared were printable, which explains the lower values of the rheological properties of the unwashed sample (Figure 7) compared to those shown in Figures 2–4. Ethanol treatments had clear, concentration-dependent effects on ink rheology. Decolorization did not change the shear-thinning behavior of the ink but significantly increased its apparent viscosity (Figure 7a), indicating that pigment removal resulted in more resistant dispersions and substantially strengthened the ink's structure. At low shear (0.10 s^{-1}), the apparent viscosity increased by approximately 66%, 162%, and 179% for the 70%, 85%, and 100% ethanol treatments, respectively, compared to the unwashed sample. This viscosity increase with ethanol concentration can be associated with more removal of chlorophyll, lipids, and other non-protein components, which likely enable tighter packing of cell wall fragments and enhance water structuring within the ink matrix.

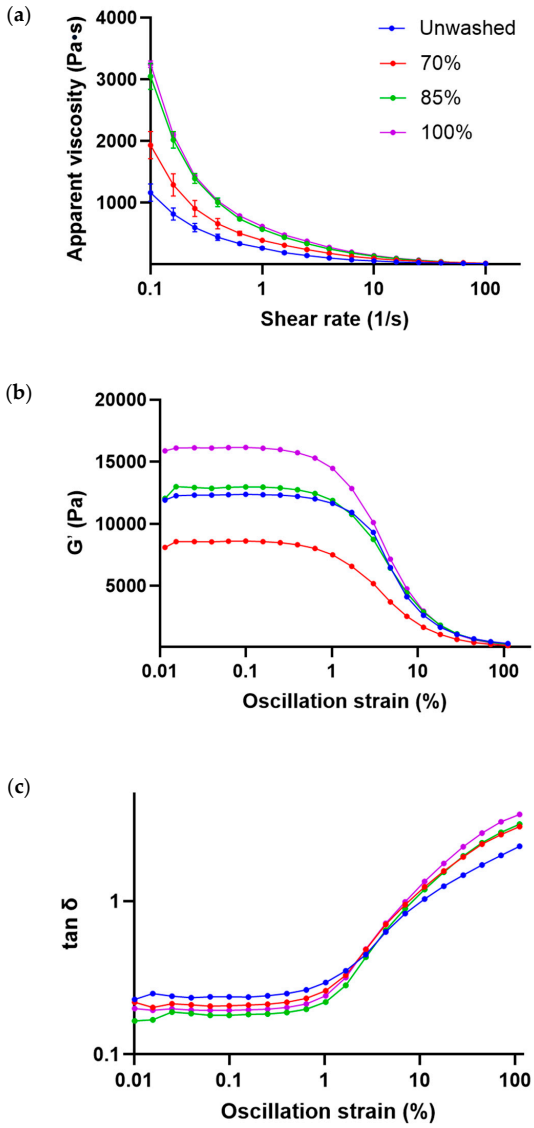


Figure 7. (**a**) Apparent viscosity, (**b**) storage modulus, and (**c**) loss factor of 3D printing inks formulated with high-pressure homogenized (20,000 psi for one pass) *C. vulgaris* decolorized by ethanol solutions of different concentrations.

Decolorized microalgae also reinforced the ink structure, as indicated by the 78%, 170%, and 235% higher G′ values within the LVR for the 70%, 85%, and 100% ethanol-treated samples, respectively, compared to the unwashed one (Figure 7b). The results imply that ethanol of higher concentration led to the formation of a more interconnected elastic network, and the effect persisted beyond the LVR. The increased G′ altered the viscoelastic balance of the ink, in terms of decreased tan δ in the LVR, by 11–23% (Figure 7c), featuring a more elastic-dominant structure. However, at high strain (17.8%), the tan δ of the decolorized microalgae-based ink became markedly higher than that of the one containing the unwashed sample, by 25%, 24%, and 41% for the treatments with 70%, 85%, and 100% ethanol, respectively, showing that once the ink strain passed its LVR, ethanol treatment made the ink dissipate more energy and behave more viscously. The viscosity and tan δ results suggest that decolorized microalgae formed a stronger elastic ink under small deformation but allowed greater viscous flow once the ink structure yielded.

3.6.4. Textural Properties and Protein Bioaccessibility of 3D Prints Comprising HPH-Treated Decolorized Microalgae

Figure 8 shows the 3D prints containing HPH-treated decolorized microalgae which had different texture profiles from the one printed with the unwashed sample, depending on the concentration of the ethanol solution used, as presented in Figure 9. Ethanol treatments in general increased the print hardness (47–128%), resilience (19–109%), springiness (−3 to 155%), and chewiness (47–408%) at different levels, while the print cohesion exhibited a concentration-dependent response, with a marked increase (77%) observed for the 100% ethanol treatment. These increases indicate that when more chlorophyll and lipophilic components were removed, the structural networks formed during printing were more integrated, self-supporting and elastic. Ethanol treatment may also induce partial protein conformational changes or dehydration-induced aggregation [42], which could further contribute to the observed increase in print hardness. Similarly, ethanol has been found to induce hardening of protein-based hydrogels with increased gumminess and chewiness [42], as well as promote network contraction within polysaccharide gel matrices to form tighter junction zones [43]. In contrast, the print adhesiveness largely decreased, by 30–58%, as the ethanol concentration increased, reflecting reduced stickiness and thus improved handling, which agrees with the lower adhesiveness of ethanol-treated gels reported by Ekumah et al. (2023) [44].

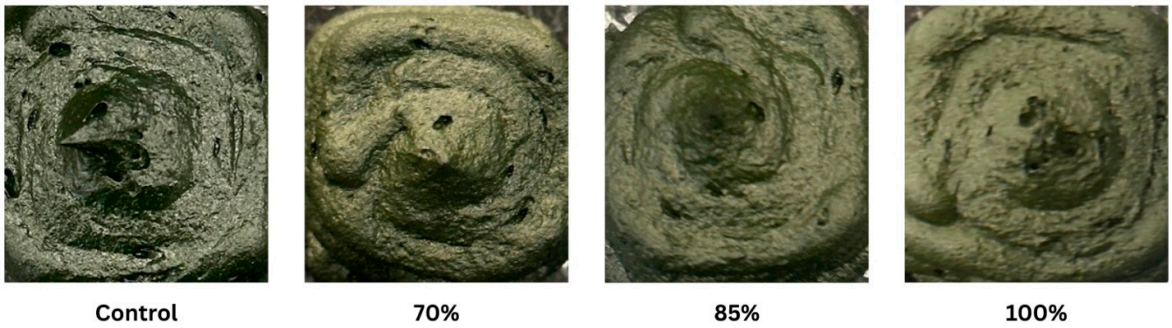


Figure 8. Images of 3D prints comprising high-pressure homogenized (20,000 psi for one pass) *C. vulgaris* decolorized by ethanol solutions of different concentrations.

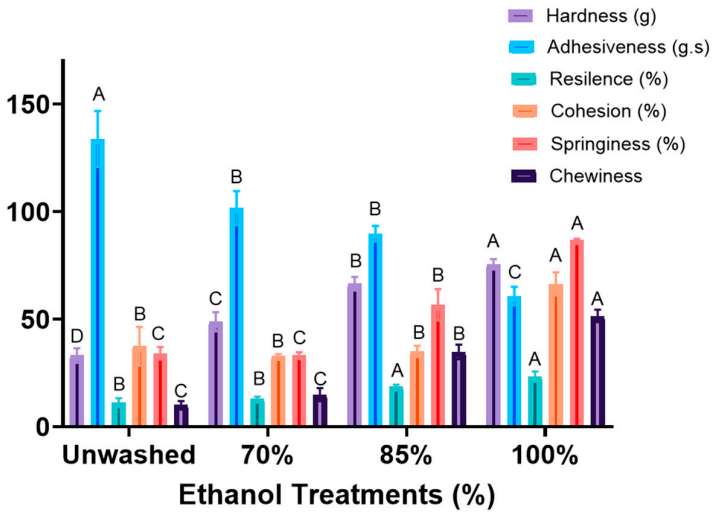


Figure 9. Texture profiles of 3D prints comprising high-pressure homogenized (20,000 psi for one pass) *C. vulgaris* decolorized by ethanol solutions of different concentrations. Bars within the same treatment group indicated with different letters have significantly different values ($p < 0.05$).

Microalgae decolorization did not result in significant differences in the protein bioaccessibility of the printed samples (Figure 10), implying that ethanol-based decolorization treatment, regardless of concentration, did not compromise protein digestibility during simulated gastrointestinal digestion.

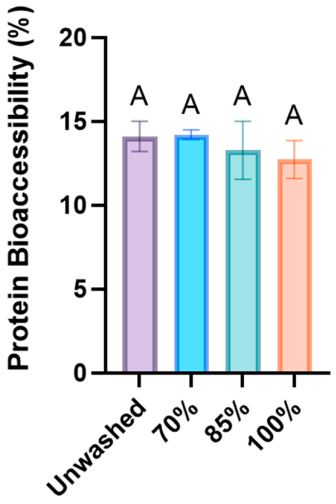


Figure 10. Protein bioaccessibility of 3D prints comprising high-pressure homogenized (20,000 psi for one pass) *C. vulgaris*, decolorized by ethanol solutions of different concentrations. Bars indicated with same letters have values showing no significant difference ($p > 0.05$).

4. Conclusions

In this study, HPH was applied at different pressures for different numbers of passes to modify *C. vulgaris* for advancing the 3D printability of microalgae-based inks. HPH treatments partially or completely disintegrate microalgal cells and increase the FS of microalgae without compromising their EAI, ESI and FC. Printing inks formulated with HPH-treated microalgae showed higher viscosity and elastic response, generally as the pressure and pass number increased. The 3D prints from inks comprising HPH-treated microalgae featured lower adhesiveness, cohesiveness and chewiness but higher resilience. Intense HPH treatments reduced the solubility of microalgae and thus the protein bioaccessibility of the prints. Chlorophyll removal through ethanol extraction effectively decolored

microalgae and also increased their WHC and solubility, allowing formulation of printing inks with higher viscosity and G′. The resulting 3D prints were stiffer, more elastic, and more structurally stable.

Overall, while HPH proved effective in altering microalgae-based ink rheology and print texture, mild treatment intensity, like 10,000 psi and/or one pass in this study, is recommended to avoid compromising microalgal protein integrity and accessibility. Additionally, microalgae decolorization can not only largely improve the visual acceptance of their derived products but also modify their functionalities for better 3D printability. The combination of these pretreatments is expected to expand the applications of microalgae in food for development of novel 3D-printed products.

Although the TPA performed in this study reveals important characteristics of the 3D prints, further evaluation on 3D printing performance is needed through analyzing extrusion force and print's filament uniformity, layer adhesion, collapse behavior, and dimensional stability. Quantifying these parameters will allow development-predictive formulation models for more accurately correlating the print properties with ink rheology and printing conditions.

Author Contributions: Conceptualization, J.-Y.H.; Methodology, D.S., A.M.-K., D.C. and J.-Y.H.; Validation, D.S.; Formal analysis, D.S.; Investigation, D.S.; Resources, D.C., S.S. and J.-Y.H.; Data curation, D.S. and J.-Y.H.; Writing—original draft, D.S.; Writing—review and editing, A.M.-K., J.A.V., D.C., S.S. and J.-Y.H.; Visualization, D.S.; Supervision, A.M.-K., J.A.V., D.C. and J.-Y.H.; Project administration, J.-Y.H.; Funding acquisition, J.-Y.H. All authors have read and agreed to the published version of the manuscript.

Funding: This work is supported by the Agriculture and Food Research Initiative, project award numbers 2023-68012-39001 and 2023-68016-39718, and Hatch project number 1014964 from the U.S. Department of Agriculture's National Institute of Food and Agriculture.

Data Availability Statement: The original contributions presented in this study are included in the article. Further inquiries can be directed to the corresponding author.

Conflicts of Interest: The authors declare no conflict of interest.

References

1. Hu, J.; Meng, W.; Su, Y.; Qian, C.; Fu, W. Emerging technologies for advancing microalgal photosynthesis and metabolism toward sustainable production. *Front. Mar. Sci.* **2023**, *10*, 1260709. [CrossRef]
2. U.S. Food and Drug Administration. *Agency Response Letter GRAS Notice No. GRN 000986: Chlorella Powder and Chlorella Micro Powder*; U.S. Department of Health and Human Services: Silver Spring, MD, USA, 2021. Available online: https://hfpappexternal.fda.gov/scripts/fdcc/index.cfm?set=GRASNotices&id=986 (accessed on 3 November 2025).
3. Bleakley, S.; Hayes, M. Algal proteins: Extraction, application, and challenges concerning production. *Foods* **2017**, *6*, 33. [CrossRef]
4. Lopes, P.A.; Coelho, D.; Prates, J.A.M. Testimony on a successful lab protocol to disrupt *Chlorella vulgaris* microalga cell wall. *PLoS ONE* **2022**, *17*, e0268565. [CrossRef] [PubMed]
5. Weber, S.; Grande, P.M.; Blank, L.M.; Klose, H. Insights into cell wall disintegration of *Chlorella vulgaris*. *PLoS ONE* **2022**, *17*, e0262500. [CrossRef] [PubMed]
6. Hussain, S.; Malakar, S.; Arora, V.K. Extrusion-based 3D food printing: Technological approaches, material characteristics, printing stability, and post-processing. *Food Eng. Rev.* **2021**, *14*, 100–119. [CrossRef]
7. Zhu, W.; Iskandar, M.M.; Baeghbali, V.; Kubow, S. Three-dimensional printing of foods: A critical review of the present state in healthcare applications and potential risks and benefits. *Foods* **2023**, *12*, 3287. [CrossRef]
8. Mirzapour-Kouhdasht, A.; Biparva, P.; McClements, D.J.; Garavand, F.; Garcia-Vaquero, M. Formulation of inks for 3D printing of microalgae-based meat analogues and the role of modified starch: A review. *Int. J. Food Sci. Technol.* **2024**, *59*, 8618–8629. [CrossRef]
9. Verni, M.; Demarinis, C.; Rizzello, C.G.; Pontonio, E. Bioprocessing to preserve and improve microalgae nutritional and functional potential: Novel insight and perspectives. *Foods* **2023**, *12*, 983. [CrossRef]
10. Mesa, J.; Hinestroza-Córdoba, L.I.; Barrera, C.; Seguí, L.; Betoret, E.; Betoret, N. High homogenization pressures to improve food quality, functionality and sustainability. *Molecules* **2020**, *25*, 3305. [CrossRef]

11. Morata, A.; Guamis, B. Use of UHPH to obtain juices with better nutritional quality and healthier wines with low levels of SO_2. *Front. Nutr.* **2020**, *7*, 598286. [CrossRef]
12. Safi, C.; Charton, M.; Ursu, A.V.; Laroche, C.; Zebib, B.; Pontalier, P.-Y.; Vaca-Garcia, C. Release of hydro-soluble microalgal proteins using mechanical and chemical treatments. *Algal Res.* **2014**, *3*, 55–60. [CrossRef]
13. Magpusao, J.; Giteru, S.; Oey, I.; Kebede, B. Effect of high pressure homogenization on microstructural and rheological properties of *Arthrospira platensis*, *Isochrysis*, *Nannochloropsis* and *Tetraselmis* species. *Algal Res.* **2021**, *56*, 102327. [CrossRef]
14. McCauley, J.I.; Winberg, P.C.; Meyer, B.J.; Skropeta, D. Effects of nutrients and processing on the nutritionally important metabolites of *Ulva* sp. (Chlorophyta). *Algal Res.* **2018**, *35*, 586–594. [CrossRef]
15. Morcelli, A.; Cassel, E.; Vargas, R.; Rech, R.; Marcílio, N. Supercritical fluid (CO_2+ethanol) extraction of chlorophylls and carotenoids from *Chlorella sorokiniana*: COSMO-SAC assisted prediction of properties and experimental approach. *J. CO_2 Util.* **2021**, *51*, 101649. [CrossRef]
16. Sun, J.; Zhou, W.; Huang, D.; Fuh, J.Y.H.; Hong, G.S. An overview of 3D printing technologies for food fabrication. *Food Bioprocess Technol.* **2015**, *8*, 1605–1615. [CrossRef]
17. Beuchat, L.R. Functional and electrophoretic characteristics of succinylated peanut flour protein. *J. Agric. Food Chem.* **1977**, *25*, 258–261. [CrossRef]
18. Pearce, K.N.; Kinsella, J.E. Emulsifying properties of proteins: Evaluation of a turbidimetric technique. *J. Agric. Food Chem.* **1978**, *26*, 716–723. [CrossRef]
19. Smith, P.K.; Krohn, R.I.; Hermanson, G.T.; Mallia, A.K.; Gartner, F.H.; Provenzano, M.D.; Fujimoto, E.K.; Goeke, N.M.; Olson, B.J.; Klenk, D.C. Measurement of protein using bicinchoninic acid. *Anal. Biochem.* **1985**, *150*, 76–85. [CrossRef]
20. Mirzapour-Kouhdasht, A.; Moosavi-Nasab, M.; Kim, Y.M.; Eun, J.B. Antioxidant mechanism, antibacterial activity, and functional characterization of peptide fractions obtained from barred mackerel gelatin with a focus on application in carbonated beverages. *Food Chem.* **2021**, *342*, 128339. [CrossRef]
21. Li, J.; Moeinzadeh, S.; Kim, C.; Pan, C.C.; Weale, G.; Kim, S.; Abrams, G.; James, A.W.; Choo, H.; Chan, C.; et al. Development and systematic characterization of GelMA/alginate/PEGDMA/xanthan gum hydrogel bioink system for extrusion bioprinting. *Biomaterials* **2023**, *293*, 121969. [CrossRef]
22. Piola, B.; Sabbatini, M.; Gino, S.; Invernizzi, M.; Renò, F. 3D bioprinting of gelatin-xanthan gum composite hydrogels for growth of human skin cells. *Int. J. Mol. Sci.* **2022**, *23*, 539. [CrossRef] [PubMed]
23. Habib, M.A.; Khoda, B. Rheological analysis of bio-ink for 3D bio-printing processes. *J. Manuf. Process.* **2022**, *76*, 708–718. [CrossRef] [PubMed]
24. Pereira, T.; Barroso, S.; Gil, M.M. Food texture design by 3D printing: A review. *Foods* **2021**, *10*, 320. [CrossRef]
25. Rodríguez-Herrera, V.V.; Umeda, T.; Kozu, H.; Kobayashi, I. Formation and texture analysis of extrusion-based 3D printed foods using nixtamalized corn and chickpea flours: Effect of cooking process. *Appl. Sci.* **2024**, *14*, 7315. [CrossRef]
26. Minekus, M.; Alminger, M.; Alvito, P.; Ballance, S.; Bohn, T.; Bourlieu, C.; Carrière, F.; Boutrou, R.; Corredig, M.; Dupont, D.; et al. A standardised static in vitro digestion method suitable for food—An international consensus. *Food Funct.* **2014**, *5*, 1113–1124. [CrossRef]
27. Katsimichas, A.; Katsouli, M.; Spantidos, N.; Giannakourou, M.C.; Taoukis, P. Effect of high-pressure homogenization on the functional and emulsifying properties of proteins recovered from *Auxenochlorella pyrenoidosa*. *Appl. Sci.* **2024**, *15*, 131. [CrossRef]
28. Folgado, C.; Pajuelo, A.; Ruiz-Carrascal, J.; Perez-Palacios, T. Bioaccessibility of EPA and DHA in microencapsulated algae oil as affected by wall material and homogenisation techniques. *Food Bioprod. Process.* **2026**, *157*, 205–216. [CrossRef]
29. Ebert, S.; Grossmann, L.; Hinrichs, J.; Weiss, J. Emulsifying properties of water-soluble proteins extracted from the microalgae *Chlorella sorokiniana* and *Phaeodactylum tricornutum*. *Food Funct.* **2019**, *10*, 754–764. [CrossRef]
30. Georgiou, D.; Charisis, A.; Theocharidou, A.; Ritzoulis, C.; Papapanagiotou, G.; Samara, C.; Chatzidoukas, C.; Kalogianni, E.P. Foaming properties of *Chlorella sorokiniana* microalgal biomass. *Colloids Interfaces* **2024**, *8*, 66. [CrossRef]
31. Han, Y.; Zhu, L.; Karrar, E.; Qi, X.; Zhang, H.; Wu, G. Pickering foams stabilized by protein-based particles: A review of characterization, stabilization, and application. *Trends Food Sci. Technol.* **2023**, *133*, 148–159. [CrossRef]
32. Van de Walle, S.; Muylaert, K.; Van Royen, G. Influence of cell disruption on techno-functional properties and digestibility of *Chlorella vulgaris* proteins. *Innov. Food Sci. Emerg. Technol.* **2025**, *102*, 104023. [CrossRef]
33. Wang, M.; Yin, Z.; Sun, W.; Zhong, Q.; Zhang, Y.; Zeng, M. Microalgae play a structuring role in food: Effect of *Spirulina platensis* on the rheological, gelling characteristics, and mechanical properties of soy protein isolate hydrogel. *Food Hydrocoll.* **2023**, *136*, 108244. [CrossRef]
34. Sow, W.J.C.; Du, J. Effects of high-pressure homogenization and ultrasound on the composition, structure, and physicochemical properties of proteins extracted from *Nannochloropsis oceanica*. *Ultrason. Sonochem.* **2024**, *105*, 106851. [CrossRef]
35. Tejada-Ortigoza, V.; Cuan-Urquizo, E. Towards the development of 3D-printed food: A rheological and mechanical approach. *Foods* **2022**, *11*, 1191. [CrossRef] [PubMed]

36. Mosibo, O.K.; Ferrentino, G.; Udenigwe, C.C. Microalgae proteins as sustainable ingredients in novel foods: Recent developments and challenges. *Foods* **2024**, *13*, 733. [CrossRef]
37. Rahman, M.M.; Hosano, N.; Hosano, H. Recovering microalgal bioresources: A review of cell disruption methods and extraction technologies. *Molecules* **2022**, *27*, 2786. [CrossRef]
38. Rahban, M.; Ahmad, F.; Piatyszek, M.A.; Haertlé, T.; Saso, L.; Saboury, A.A. Stabilization challenges and aggregation in protein-based therapeutics in the pharmaceutical industry. *RSC Adv.* **2023**, *13*, 35947–35963. [CrossRef]
39. Grossmann, L.; Hinrichs, J.; Weiss, J. Solubility and aggregation behavior of protein fractions from the heterotrophically cultivated microalga *Chlorella protothecoides*. *Food Res. Int.* **2019**, *116*, 283–290. [CrossRef]
40. Ursu, A.-V.; Marcati, A.; Sayd, T.; Sante-Lhoutellier, V.; Djelveh, G.; Michaud, P. Extraction, fractionation and functional properties of proteins from the microalgae *Chlorella vulgaris*. *Bioresour. Technol.* **2014**, *157*, 134–139. [CrossRef]
41. Feng, Y.; Ma, X.; Kong, B.; Chen, Q.; Liu, Q. Ethanol induced changes in structural, morphological, and functional properties of whey protein isolates: Influence of ethanol concentration. *Food Hydrocoll.* **2021**, *111*, 106379. [CrossRef]
42. Kleemann, C.; Zink, J.; Selmer, I.; Smirnova, I.; Kulozik, U. Effect of ethanol on the textural properties of whey protein and egg white protein hydrogels during water-ethanol solvent exchange. *Molecules* **2020**, *25*, 4417. [CrossRef]
43. Song, Q.; Wu, L.; Li, S.; Zhao, G.; Cheng, Y.; Zhou, Y. Aggregation of konjac glucomannan by ethanol under low-alkali treatment. *Food Chem. X* **2022**, *15*, 100407. [CrossRef]
44. Ekumah, J.-N.; Han, X.; Liang, Q.; Kang, L.; Wei, B.; Rashid, A.; Virk, M.S.; Qayum, A.; Adade, S.Y.-S.S.; Johnson, N.A.N.; et al. Production of kudzu starch gels with superior mechanical and rheological properties through submerged ethanol exposure and implications for in vitro digestion. *Foods* **2023**, *12*, 3992. [CrossRef]

Disclaimer/Publisher's Note: The statements, opinions and data contained in all publications are solely those of the individual author(s) and contributor(s) and not of MDPI and/or the editor(s). MDPI and/or the editor(s) disclaim responsibility for any injury to people or property resulting from any ideas, methods, instructions or products referred to in the content.